



Structural and Optical Properties of (MgZnO/rGO) Nanocomposites

Gunja Lavanya¹, Thirukachhi Suvarna¹, C. P. Vardhani^{1,*}

¹Department of Physics, Osmania University, Hyderabad-500007, India.

ARTICLE INFO

Article history:

Received 8 May 2023

Received in revised form 15 July 2023

Accepted 18 July 2023

Available online 30 September 2023

Keywords:

Nanocomposites
 MgZnO/rGO
 Co-Precipitation
 Structural
 Optical properties

ABSTRACT

Magnesium-Zinc oxide/Reduced Graphene Oxide (MgZnO/rGO) nanocomposites have been successfully synthesized by the Co-precipitation process. Obtained materials were characterized by the X-ray diffraction (XRD) shows both the hexagonal wurtzite structure of ZnO crystal planes and cubic structure of MgO. This fact shows that the prepared samples are not a single phase but a composite. Peak broadening indicates that the smaller crystallites size of the prepared MgZnO/rGO nanocomposites. The structural morphology was studied by Field emission Scanning electron microscope (FESEM) shows that the nanoparticles are connected with each other to form agglomerated granular structure which may be due to the high surface to volume ratio that results in high surface energy and the elemental analysis is confirmed by Energy dispersive X-ray analysis (EDAX) shows four strong peaks correspond to carbon (C), oxygen (O), zinc (Zn) and magnesium(Mg) with different weight percentages by doping Mg at different compositions. The functional groups of the samples are confirmed by the Fourier-transform infrared spectroscopy (FTIR) observed in the spectra at nearly ~3685 due to the O-H Stretching vibrations, peaks observed at ~2860 due to the C-H stretching vibrations, 1596-1545 due to the C=O stretching vibrations. The strong bands located at 746 and 530 cm^{-1} indicate the stretching vibration mode of Mg-O and Zn-O, respectively, which confirm the formation of MgZnO/rGO nano composites. The optical properties of the prepared MgZnO/rGO samples are characterized by the UV-visible absorption to determine the band gap of the metal oxide nanocomposites. It can be seen in all the spectra that the strong absorption peaks were appeared at around 350 nm, which is attributed to the band gap absorption in MgZnO nanocomposites. The calculated values of the band gap energies of MgZnO nanocomposites are 3.47, 3.48 and 3.51 eV respectively, at wavelengths 357nm, 356nm and 352nm which are good agreement with reported band gap values of MgZnO nanocomposites. Most studies have been concentrated on thin films; synthesis and study of MgZnO nanocomposites are rare. MgZnO/rGO nanocomposites are mainly applicable in various electrical, optoelectronic and photo catalytic applications. In the present study, Mg-doped ZnO/rGO with different Mg compositions was prepared by Co-precipitation method with subsequent calcination at high temperature. Crystalline structure, morphology and optical properties were investigated and discussed according to the experimental results.

* Corresponding author. e-mail: vardhani_c2001@yahoo.co.in

<https://doi.org/10.22034/JCHEMLETT.2023.396420.1116>



This work is licensed under [Creative Commons license CC-BY 4.0](https://creativecommons.org/licenses/by/4.0/)

1. Introduction

Now a days the world demanding a material that should possess inherent properties like larger band gap and higher electron mobility. So on making investigation about such a material the name of the compound comes out i.e. Zinc Oxide (ZnO) which is a wide gap semi conductor material well satisfying the above required properties. Recent works on Mg doped ZnO nanoparticles shows the immense potential of the ZnO based devices in future. Mixed metal oxides have found increasing research focus and applications in physics, chemistry, materials science and engineering. The combination of two or more metals in an oxide matrix can produce materials with a novel physical and chemical properties leading to relatively higher performance in various technological applications. During the last few years, synthesis of metal oxide nanocomposites materials have been attracted considerable attention [1–4]. The metal oxides nanocomposites are important technological materials for use in electrical, optoelectronic and photonic devices and as catalysts in chemical industries. A wide range of various metal oxide semiconductors have a great potential in practical applications [5]. Recently graphene oxide (GO) has gained a lot of interest as an alternative and efficient way to produce graphene. In the nearly 20 years since fullerenes and carbon nanotubes, scientists found later, three-dimensional diamond, two-dimensional graphite, one-dimensional carbon nanotubes, zero-dimensional fuller ball full carbon-based family [6] [7]. Therefore, A. K. Geim and K. Novoselov also won the Nobel Prize in Physics in 2010, because the graphene was discovered [8-9]. Besides its use for graphene production, its large surface area and presence of oxygen containing functional groups [10], [11], [12] have also raised interest for various electrical, electronic, optoelectronic and photo catalytic applications. Graphene oxide consists of few layers of graphene with epoxy and hydroxyl groups attached to the carbon atoms in the basal plane while carboxyl and carbonyl groups are attached to the edges of the sheet [13]. Graphene oxide is thus hydrophilic due to the presence of the functional groups and it can be easily dispersed in aqueous or organic solvents [14]. Despite the fact GO is considered to be an insulator, the conductivity can be partially restored by removing the functional groups through several reduction processes extensively reported in the literature [11],[12], [14], [15], [16], [17]. Among them, reduced graphene oxide (rGO) has been successfully produced by chemical, thermal and electrochemical reduction [11], [15]. In the chemical reduction process, hydrazine is the most commonly used reducing agent; however it can contaminate the final product and is also harmful for human beings and the environment. The thermal reduction process

requires high temperature, which makes it not suitable for flexible substrates. The Hummers method, even though quite cheap and environmental friendly, makes large scale production of graphene. Nano crystalline zinc oxide (ZnO), an n-type metal oxide semiconductor, is one of the metal oxides which comprises wide band gap energy of 3.37 eV, large excitation binding energy of 60 meV along with good optical, electrical, and piezoelectric responses [18]. Zinc oxide (ZnO) is a wide band gap n-type semiconductor with an energy gap of 3.37 eV at room temperature. It has been used considerably for its catalytic, electrical, optoelectronic, and photochemical properties. MgO is typical wide band gap semiconductor; it possesses unique optical, electronic, magnetic, thermal, mechanical and chemical properties due to its characteristic structures [19]. These two oxides have been widely used in almost the same application areas. Developing a new composite material by combining them into one could open up a new direction for research and applications [20-22]. It is well known that graphene sheet possesses unique two-dimensional layer structure of sp²-hybridized carbon atoms [23], which exhibits novel electronic property as a zero-band gap semiconductor and highly electronically conductivity for storing and transporting electrons. Nowadays, graphene-based nanocomposites have attracted significant attention because of these unique properties [24-30]. Compared with the pure ZnO material [31], ZnO-reduced graphene oxide (ZnO-RGO) nanocomposites can improve numerical applications. In recent years, researchers have focused more on the synthesis of nanocomposites of MgZnO/rGO due to their application in advanced technologies. Various physicochemical techniques have been employed to construct nano sized MgZnO/rGO nanoparticles [32-40]. The previous studies indicated that Mg-doped ZnO-RGO nanocomposites had a huge potential application of photoelectric device [41, 42], [43]. Several techniques have been also developed to prepare nanocomposite of MgZnO/rGO. This nanocomposite has attracted much attention because it has a larger band gap than ZnO [44-46]. However, most of the techniques need high temperatures and perform under a costly inert atmosphere. Our goal in this research is to suggest an easy method to synthesize magnesium zinc oxide/reduced graphene oxide nanocomposites. Considering the importance of semi conducting materials in materials science and future battery applications, the present work is focused on the synthesis of magnesium Zinc oxide/reduced graphene oxide (MgZnO/rGO) nanocomposites. They have attracted increasing interest in fabricating nanostructures with the size and the optical properties could be achieved. With this motivation, MgZnO/rGO nanocomposites were prepared by simple Co-

precipitation process and their structural, size and optical properties were studied. The synthesized samples are subjected to the different characterization techniques such as the powder X-Ray Diffraction (XRD), SEM, the Fourier Transform Infrared (FTIR), the Ultraviolet-visible (UV-vis) absorption studies. Most studies have been concentrated on thin films; synthesis and study of MgZnO nanocomposites are rare. In the present study, Mg-doped ZnO with different Mg contents was prepared by Co-precipitation method. Compared to other physical and chemical-based synthesis methods the Co-precipitation process advantages and disadvantages are mentioned below

CO-precipitation advantages

Simple and rapid preparation

Easy control of particle size and composition

Low temperature

Energy efficient

Disadvantages

Trace impurities may also get precipitated with a product

Time consuming

Batch-to-batch reproducibility problems

Several factors, such as pH of the reaction mixture, calcinations temperature, reaction time, stirring speed and concentration of metal precursors, greatly affect the properties of the zinc oxide nanoparticles and ZnO/rGO nanocomposite. Reaction time, reaction temperature and calcinations temperature influence the crystallite size of ZnO nanoparticles. Crystalline structure, morphology and optical properties were investigated and discussed according to the experimental results.

2. Experimental Part

2.1. Synthesis of Graphene oxide (GO) and reduced graphene oxide (rGO)

For the graphene oxide preparation, the modified Hummers' method [47] was followed. 3g of natural graphite powder, 1.5g of NaNO₃ (99%, Sigma Aldrich) and 100 ml of H₂SO₄ (99%, Sigma Aldrich) were mixed and the mixture was stirred for 5 hours at 450 rpm in an ice bath. Then, 6g of KMnO₄ (99%, Sigma Aldrich) was added slowly to the above mixture and stirred at room temperature for 36h. The large amount of heat evolution was observed during this reaction. After stirring, 250ml of double distilled water was added below 25 degrees. Then, 5ml of H₂O₂ was added to the solution. The color of the solution was changed from dark brownish to light yellow color. Then the combined mixture was stirred for 6h and aged for 24 h. The slurry was washed using 5% HCL to remove impurities. Then they obtained product was washed with DI water several times to obtain the neutral pH. The slurry was washed with ethanol for 2-3 times. The washed product was dried in a vacuum oven at 333 K for 24 pH. The dried

powder was ground using an agate mortar to get fine powder of graphene oxide (GO). A mixture of 1.5g of GO powder and 500ml of DI water was prepared. The mixture was stirred for 30 minutes to form the GO dispersion. Next 1ml of hydrazine hydrate was added in to the dispersion. The mixture was heated to 80 degrees and stirred for 72 hours. After 72 hours the mixture was transferred in to 6 different 50ml centrifuge tubes for cleaning. The cleaning was done by adding DI water and centrifuged at 5000rpm for 15 minutes. These steps were repeated twice before dry in an oven at 80 degrees for 24 hours. Finally the resultant product was obtained (rGO).

2.2. Synthesis of MgZnO/rGO nanocomposites

The magnesium zinc oxide/reduced graphene oxide nanocomposites were prepared by the co-precipitation process. All the chemical reagents were purchased from sigma Aldrich and used directly without further purification. Mg_xZn_{1-x}O powders with (x=0, 0.03, 0.06, 0.09) grams were prepared using 100 mL of distilled water, metal nitrates and sodium hydroxide. 100 mL of zinc nitrate mixed with magnesium nitrate solution was stirred well for 30 minutes at 70 degrees. Further 3.8 grams of sodium hydroxide was dissolved in 100 mL of distilled water and added to the metal nitrate solution slowly till it reaches the pH ~8 and stirred at 70 degrees at 550 rpm for 3 hours, the obtained solution was washed and filtered and dried in an oven at 160 degrees for 3 hours and calcinated at 250 degrees. The obtained powder was ground using mortar and pestle and collected. In the same procedure the other samples of different compositions were prepared. The obtained Mg_xZnO_(1-x) (x=0, 0.03, 0.06 and 0.09) nanocomposites are added to the GO solution (0.02 grams of reduced graphene oxide is added in a 100 ml of distilled water) and stirred at 30 minutes on a magnetic stirrer, the obtained solutions were washed and filtered and dried in an oven at 160 degrees for 3 hours. Then, ash colored MgZnO/rGO samples was obtained, was dried and calcined at 250°C for 3h. The same procedure was followed for the preparation of Mg_xZnO_(1-x)/rGO nanocomposites in different compositions. Here, we can observe the structural, morphological and optical changes by changing the magnesium doping concentrations.

3. Characterizations

The characterization of metal oxide nanocomposites is essential for understanding of their structural and optical properties. Development of novel tools and instruments are one of the greater challenges in nanotechnology. The prepared samples were characterized by using various physicochemical methods namely XRD, SEM, EDAX, FTIR, and UV-vis. The prepared MgZnO/rGO samples

were characterized by using the powder X-ray ($\lambda=0.15496$ nm). The structures of the samples were studied by using the FESEM. The presence of elements in the compound was recorded using the ZIESS ULTRATM-55 Instrument attached to the FESEM. The FTIR spectrum of the prepared sample was recorded, with Cuk resolution of 4 cm^{-1} over the range $4000\text{--}400\text{ cm}^{-1}$. The absorption study of the prepared samples has been carried out using the UV-vis spectrophotometer.

3. Result and Discussion

3.1. XRD analysis

X-ray diffraction (XRD) is an analytical technique mainly used for the phase identification of a crystalline material, and it can provide information on unit cell dimensions. This method uses a monochromatic source of X-rays and measures the pattern of diffracted radiation, which is a result of the constructive interference due to the crystalline structure of the powder. The crystallite size can be obtained either by direct computer simulation of the X-ray diffraction pattern or from the Full Width at Half Maximum (FWHM) of the diffraction peaks using the Debye-Scherrer's formula [48].

$$D = k\lambda/\beta \cos \theta$$

Where, λ - Wavelength of X-rays, or β - FWHM in radian, θ - Peak angle. Figure 1 shows the XRD patterns of MgZnO/rGO nanocomposites. All the peaks in the patterns could be indexed to the MgZnO/rGO nanocomposites. The values located at 31.80° , 34.48° , 36.44° , 47.53° and 67.96° θ existence of strong diffraction peaks at corresponding to (100), (002), (101), (102) and (112) hexagonal wurtzite structure of ZnO crystal planes (JCPDS Card No.79-205) and peaks at 42.06° , 47.6° , 62.84° and 77.01° , corresponding to (001), (100), (102) and (110) cubic structure of MgO crystal planes (JCPDS Card No. 45-0946), respectively [49]. The three prominent peaks are

observed at $2\theta=31.80^\circ$, 34.48° , 36.44° as per JCPDS card no. 36-1451. The lowest intensity peaks are observed at $2\theta=47.6^\circ$, 56.7° , 62.84° and 67.97° . The characteristic XRD peaks of MgZnO observed in our studies are well in agreement with previous reports. This fact indicates that the prepared samples are not a single phase but a composite. Peak broadening indicates that the smaller crystallites size of the prepared MgZnO/rGO nanocomposites. Addition of magnesium has not produced any additional peak showing the formation of single phase. However, intensity of the peaks has fairly reduced particularly in the composite. In any preparation of nanomaterials, the solvent is an important parameter for determining the crystal size [50-51]. In the present work, the figure 1 shows a slight broadening of peaks. As the magnesium composition is increased from 0.03 to 0.09 the crystallite sizes are observed to be decreased. Using Scherrer's formula, the average crystallite sizes of the MgZnO/rGO samples synthesized are found to be 28.2, 28.0 and 25.4 nm respectively. This can be explained as the radius of Mg^{+2} being smaller than that of the Zn^{+2} . Increasing of Mg content decreases nano particle size of the products. The average crystallite sizes of MgZnO/rGO nanocomposites are smaller than that of the ZnO. Whereas the average crystallite size of the ZnO and ZnO/rGO are 8.46nm and 8.563nm. Figure 1 shows the major XRD peak shift for ZnO nanoparticles with different contents of Mg dopant. When Mg^{2+} ions substituted for Zn^{2+} ions in ZnO lattice, the lattice constant tends to decrease owing to the smaller ionic radius of Mg^{2+} comparing with Zn^{2+} radius. Thus the diffraction peaks shifted towards the higher diffraction angle. The intensity of all the diffraction peaks decreases as the doping concentration of Mg increases with peak broadening and there is no additional peak of MgO was observed. This indicates that the presence of Mg concentration in impurity level.

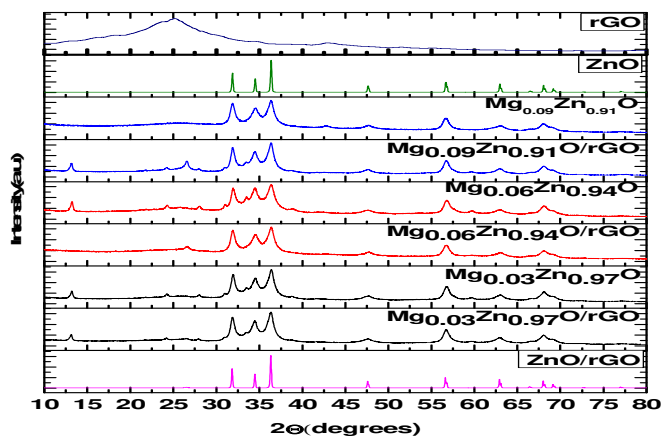


Fig 1. XRD of MgZnO/rGO nanocomposites

Table 1 shows the crystallite size, strain and dislocation intensity of MgZnO/rGO nanocomposites

S.No	Sample code	2 θ	FWHM	Crystallite size (D) (nm)	Strain	Dislocation Intensity
1	rGO	24.20027	14.54722	1.0	56.896	96.22967
2	ZnO	36.36403	0.19539	78	0.742	0.01639
3	ZnO/rGO	36.31973	0.17843	85	0.678	0.01367
4.	Mg _{0.03} Zn _{0.97} O/rGO	34.6811	5.37555	2.82	20.68	0.1275
5.	Mg _{0.06} Zn _{0.94} O/rGO	34.7060	5.41679	2.80	20.52	0.1257
6.	Mg _{0.09} Zn _{0.91} O/rGO	34.57745	5.96833	2.54	22.79	0.1550

3.2. Field Emission scanning electron microscopy (FESEM)

The surface morphology of the prepared nanomaterials was studied using field emission scanning electron microscopy as shown in Fig.2. FESEM images of MgZnO/rGO nanocomposites a-b shows Mg_xZnO_(1-x)/rGO at x= 0.03, c-d shows Mg_xZnO_(1-x)/rGO at x=0.06, e-f shows Mg_xZnO_(1-x)/rGO at x=0.09 g shows ZnO/rGO h shows ZnO and i shows rGO FESEM. It is observed that the nanoparticles are connected with each other to form agglomerated granular structure which may be due to the high surface to volume ratio that results in high surface energy. FESEM images show the disordered irregular nanoscale spherical aggregates with a narrow size distribution. However, these nanoparticles are well interconnected that helps the transportation of charge carriers over the surface [52]. The ZnO (Fig h) sample shows the formed large spherical shaped structure due to the agglomerated ZnO nanoparticles. These micro particles are formed due to the agglomeration of nanoparticles. The rGO sample is severely agglomerated because of its high specific surface area. In ZnO/rGO nanocomposite, it is observed that the ZnO nanoparticles are less agglomerated with very small amount of ZnO rods like structures [53] Due to the

agglomeration of the ZnO nanoparticles, the average diameter size of the ZnO nanoparticles in pure sample is relatively larger than the composite. In the presence of rGO, the ZnO nanoparticles are anchored onto the rGO by interacting with the residual functional groups of rGO thereby the agglomeration of the particles is relatively decreased in the composite compared to pure ZnO material. In addition, some of the ZnO nanoparticles entered into the interlayer of GO sheets form a sandwich composite structure preventing the stacking sheets. Hence, a large number of ZnO nanoparticles were observed to be densely distributed on the GO surface. When we add 3% of Mg (i.e. Mg=0.03 g) dopant we can observe the flake like structure, if we go on increasing the Mg composition the we can observe the spherical like structure which shows the formation of the MgZnO nanocomposites at different compositions .At 9% Mg dopant we can see the clearly spherical image formation of MgZnO nanocomposites within the range of 100nm and we can see that in all nanocomposites the image formation is seemed to be those are closely packed.

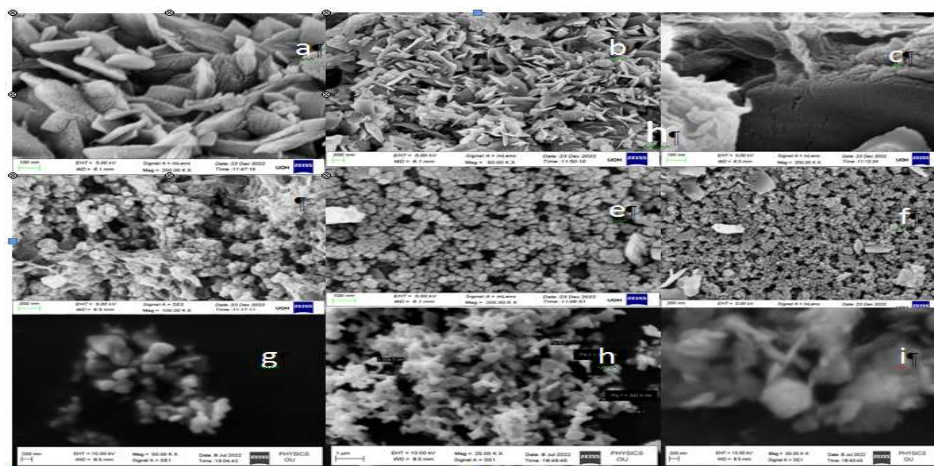


Fig 2. FESEM images of MgZnO/rGO nanocomposites a and b shows Mg_xZnO_(1-x)/rGO at x= 0.03,c and d shows Mg_xZnO_(1-x)/rGO at x=0.06,e and f shows Mg_xZnO_(1-x)/rGO at x=0.09 g shows ZnO/rGO h shows ZnO and i shows rGO FESEM images.

3.3.EDAX

The elemental composition of MgZnO/rGO nanocomposites was confirmed by FESEM with energy dispersive X-ray analysis (EDAX). The EDAX spectrum of $Mg_xZnO_{(1-x)}$ /rGO at $x=0.03$ shows four strong peaks correspond to carbon (C), oxygen (O), zinc (Zn) and magnesium(Mg).The EDAX spectrum confirmed the presence of C, O, Zn and Mg with 23.72, 30.84,31.21 and 14.23wt%, respectively. Moreover, there are no other peaks were found in the spectrum as shown in Fig. 3a, which confirms the purity of the prepared nanocomposite material. The EDAX spectrum of ($Mg_xZnO_{(1-x)}$)/rGO at $x=0.06$ shows four strong peaks correspond to carbon (C), oxygen (O), zinc (Zn) and magnesium(Mg).The EDAX spectrum confirmed the presence of C, O, Zn and Mg with 37.32, 23.47,37.56 and 1.65wt%, respectively.). The EDAX spectrum of $Mg_xZnO_{(1-x)}$ /rGO at $x=0.09$ shows four strong peaks correspond to carbon (C), oxygen (O), zinc (Zn) and magnesium(Mg).The EDAX spectrum confirmed the presence of C, O, Zn and Mg with 25.27, 23.72,48.45 and 1.57wt%, respectively. The

analysis

EDAX spectrum of rGO/ZnO nanocomposites shows three strong peaks correspond to carbon (C), oxygen (O), zinc (Zn) and two peaks related to Zn were observed at high energy region. The EDAX spectrum confirmed the presence of C, O and Zn with 49.13, 28.92 and 13.28 wt%, respectively. Moreover, there are no other peaks were found in the spectrum as shown in Fig. 3, which confirms the purity of the prepared nanocomposite material. The EDAX spectrum of ZnO nanocomposites shows two strong peaks correspond to oxygen (O) and zinc (Zn). The EDAX spectrum confirmed the presence of O and Zn with 52.02 and 47.98 wt%, respectively. From EDAX we can see that as we increase the dopant composition the atomic and weight percentages of the sample varies according to it and it shows the presence of all the elements indicates the formation of MgZnO nano composites .There are no other impurity elements are observed in the formation of MgZnO nanocomposites.

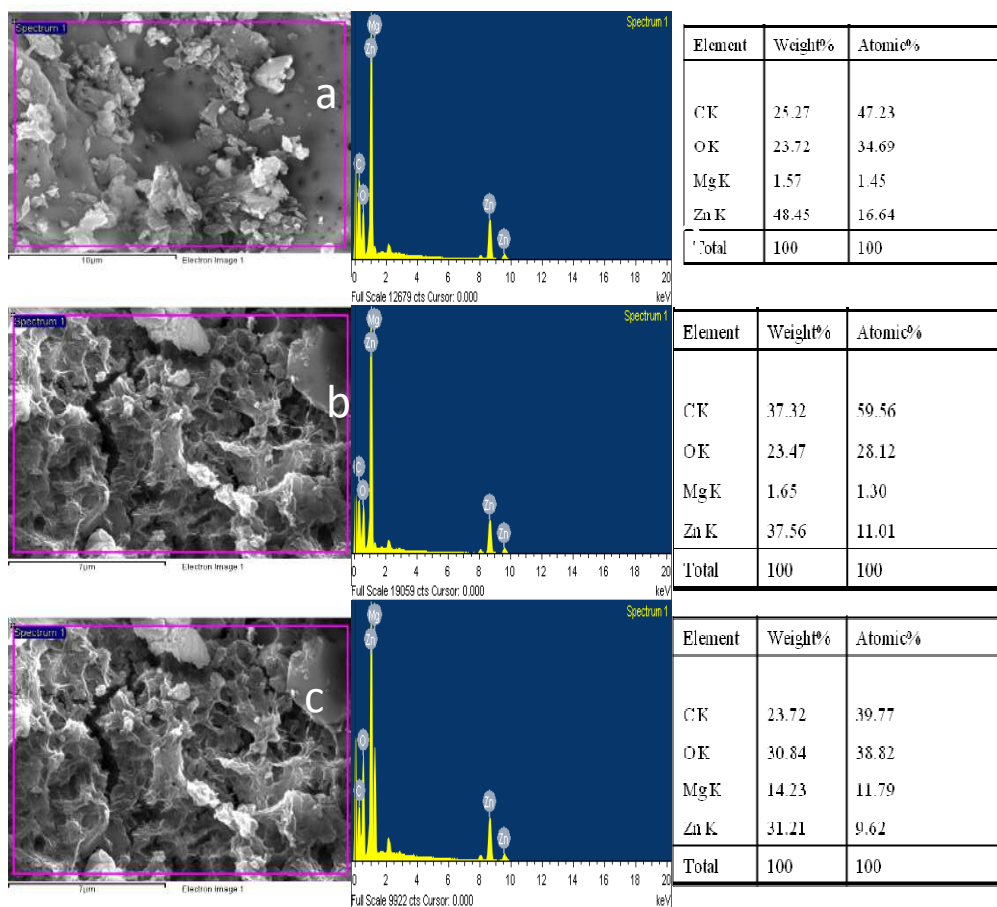


Fig 3. EDAX analysis of MgZnO/rGO nanocomposites a shows $Mg_xZnO_{(1-x)}$ /rGO at $x=0.03$, b shows $Mg_xZnO_{(1-x)}$ /rGO at $x=0.06$, c shows $Mg_xZnO_{(1-x)}$ /rGO at $x=0.09$ d shows ZnO/rGO e shows ZnO and f shows rGO EDAX analysis.

Table 2 shows the elemental composition of MgZnO nanocomposites.

S.No	Sample code	Zn		Mg		Oxygen		Carbon	
		(at%)	(wt%)	(at%)	(wt%)	(at%)	(wt%)	(at%)	(wt%)
1	rGO	-	-	-	-	36.25	38.8	56.33	45.27
2.	ZnO	81.58	52.02	-	-	18.42	47.98	-	-
3	ZnO/rGO	3.19	13.28	-	-	28.97	28.41	64.18	49.13
4	Mg _{0.03} Zn _{0.97} O/rGO	16.64	48.45	1.45	1.57	34.69	23.72	47.23	25.27
5	Mg _{0.06} Zn _{0.94} O/rGO	11.01	37.56	1.30	1.65	28.12	23.47	59.56	37.32
6	Mg _{0.09} Zn _{0.91} O/rGO	9.62	31.21	11.79	14.23	38.82	30.84	39.77	23.72

3.4. FTIR Spectra

FTIR is a powerful tool for identifying the types of chemical bonds (functional groups) in a molecule by producing an infrared absorption spectrum that is like a molecular "fingerprint". The wavelength of the light absorbed is characteristic of the chemical bond as can be seen in this spectrum. Figure 4 represents the FTIR spectrum of the peaks observed in the spectra at nearly ~3685 due to the O-H Stretching vibrations, peaks observed at ~2860 due to the C-H stretching vibrations, 1596-1545 due to the C=O stretching vibrations. The band appeared at

1054 cm⁻¹ was assigned to the C-N stretching vibration. The prominent peak observed at 581 cm⁻¹ corresponds to weak Zn-O stretching. The FTIR spectra show the prominent peaks which correspond to MgZnO as reported in the previous work [54]. Generally, the metal oxides give absorption bands below 1000 cm, arising due to the inter-atomic vibrations. Further, the strong bands located at 746 and 530 cm⁻¹ indicate the stretching vibration mode of Mg-O and Zn-O, respectively, which confirm the formation of MgZnO/rGO nano composites.

Table 3 shows the Band assignments of MgZnO/rGO nano composites.

S.No	Wave number (cm ⁻¹)	Band assignment
1.	~3685	O-H stretching vibration
2.	~2860	C-H stretching vibration
3.	1596-1545	C=O stretching vibration
4.	1054	C-N stretching vibration
5.	746	Mg-O
6.	581	Zn-O
7.	530	Zn-O weak

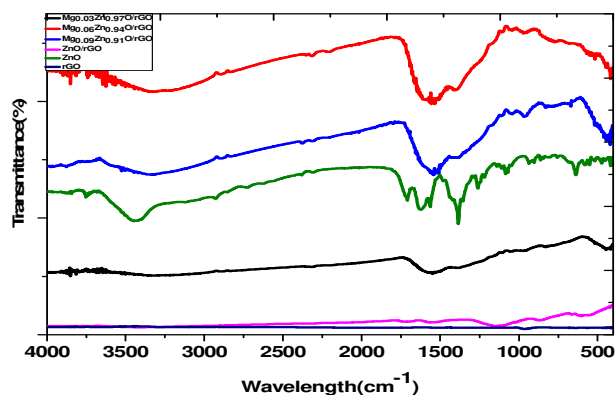


Fig.4 FTIR analysis of MgZnO/rGO nanocomposites

3.5. UV- Vis Spectra Figure 5 shows the UV-vis absorption spectrum of the ZnMgO/rGO nanocomposites prepared in different compositions respectively. It can be seen in all the spectra that the strong absorption peaks were appeared at around 350 nm, which is attributed to the band gap absorption in MgZnO nanocomposites. The addition of Mg as dopant shifts the absorption wavelength towards the lower side. The calculated values of the band gap energies of MgZnO nanocomposites are 3.47, 3.48 and 3.51 eV respectively, at wavelengths 357nm, 356nm and 352nm which are good agreement with reported band gap values of MgZnO nanocomposites. This indicates the stronger interaction between the dopant and the ZnO nanoparticles. The intensity of absorption also increases with increase in the concentration of dopant. Band gap energies of the synthesized nanoparticles were calculated by the following relation,

$$E_g = (1240/\lambda) \text{ eV}$$

λ - Wavelength of nanoparticles.

Moreover, MgO is more ionic compared to ZnO, because of 3s energy level in Mg and 4s energy level in Zn. Consequently, the energy difference between these s levels and O 2p level is smaller in ZnO and larger in MgO. Thus, ionicity is lowest in ZnO and largest in MgO. This is now

consistent with larger band gaps for MgZnO as compared to ZnO where the band gap of ZnO is 3.14eV at wavelength of 394 nm. It can be found that the absorption intensities in the visible ranges for the nano hybrids doping with or without Mg, are higher than those of pure metal oxide nanoparticles, indicating that rGO is helpful for electrons of conduction band transferring from ZnO nanoparticles to RGO itself. In the ultraviolet part, there is a slight blue-shift caused by the hybrid of RGO sheets, which is considered as the electrons accumulated near the conduction band [55]. Fig 5 describes the absorption spectra of MgZnO/rGO nanoparticles with different Mg-doped concentrations. With Mg-doped concentration increasing from 0.03, 0.06 and 0.09, the absorption peak sequentially shifts to blue, similar as authors' earlier study [56]. This phenomenon indicates that doping Mg^{2+} into ZnO increases the width of the band gap effectively. In the visible range, among the samples with different Mg-doped concentration, the absorption of $Mg_xZn_{(1-x)}/rGO$ at $X=0.09$ shows the highest absorption properties in the visible range. From the UV-vis analysis when the Mg composition is increased we can observe the change in energy band gap and wavelength as the Mg composition increases the band gap energy increases and the wavelength decreases.

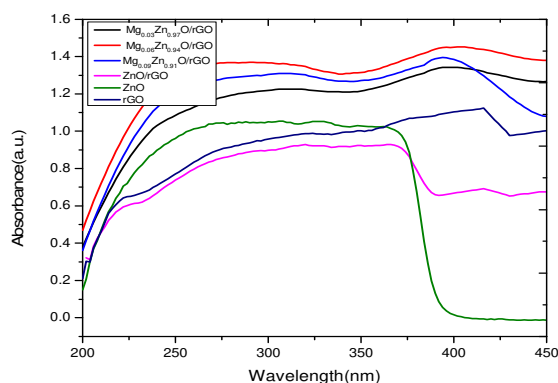


Fig 5. The UV-vis absorption spectrum analysis of MgZnO/rGO nanocomposites

Table 4 shows the Band gap energy of MgZnO/rGO nano composites.

S. No	Composition	Wavelength (nm)	Band gap energy(eV)
1	ZnO	385	3.20
2	ZnO/rGO	394	3.14
3	Mg _{0.97} Zn _{0.03} O/rGO	357	3.47
4	Mg _{0.94} Zn _{0.06} O/rGO	356	3.48
5	Mg _{0.91} Zn _{0.09} O/rGO	352	3.51

3.6. Tauc plot

Figure 6 shows the Tauc plots for the UV-vis absorption spectrum of the ZnMgO/rGO nanocomposites prepared in different compositions respectively. It can be seen in all the spectra that the strong absorption peaks were appeared at around 350 nm, which is attributed to the band gap absorption in MgZnO nanocomposites. The calculated

values of the band gap energies of MgZnO nanocomposites are 3.47, 3.48 and 3.51 eV respectively, at wavelengths 357nm, 356nm and 351nm which are good agreement with reported band gap values of MgZnO nanocomposites. From the Tauc plot we can observe that when the Mg composition is increased we can observe the change in energy band gap, as the Mg composition increases the band gap energy increases.

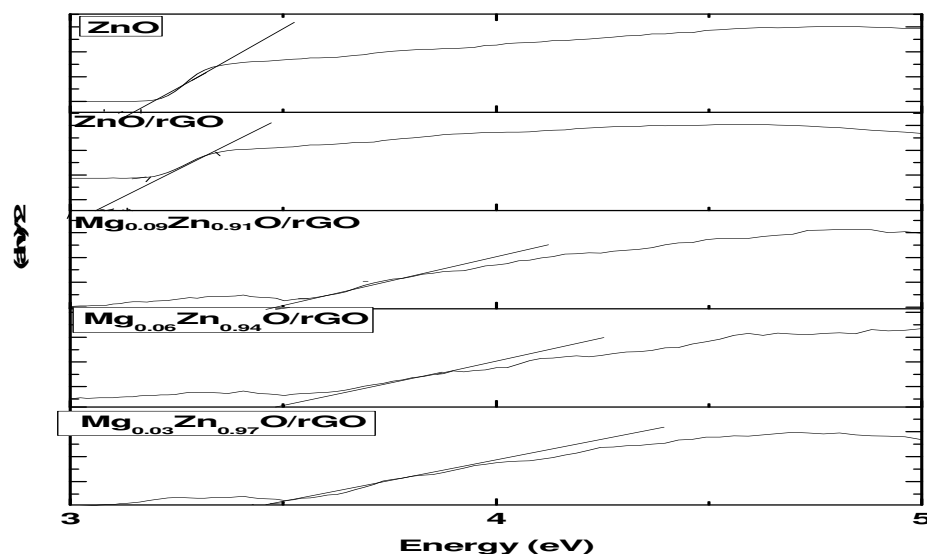


Fig 6. Tauc plots of the UV-vis absorption spectrum of MgZnO/rGO nanocomposites

4. Conclusion

Magnesium-Zinc oxide/Reduced Graphene Oxide (MgZnO/rGO) nanocomposites have been successfully synthesized by the Co-precipitation process. Obtained materials were characterized by the X-ray diffraction (XRD), Field emission Scanning electron microscope (FESEM), Energy dispersive X-ray analysis (EDAX), Fourier-transform infrared spectroscopy (FTIR) and Ultraviolet-visible spectroscopy (UV-Vis) analysis. XRD is

used to determine the structure, crystallite size and the phase of the synthesized MgZnO/rGO nanocomposites. The XRD of MgZnO/rGO nanocomposites shows both the hexagonal wurtzite structure of ZnO crystal planes and cubic structure of MgO. This fact indicates that the prepared samples are not a single phase but a composite. Peak broadening indicates that the smaller crystallites size of the prepared MgZnO/rGO nanocomposites. The structural morphology was studied by FESEM and the

elemental analysis is confirmed by EDAX. FESEM shows the nanoparticles are connected with each other to form agglomerated granular structure which may be due to the high surface to volume ratio that results in high surface energy. It shows the disordered irregular nanoscale semi-spherical aggregates with a narrow size distribution. However, these nanoparticles are well interconnected that

helps the transportation of charge carriers over the surface. The EDAX spectrum of $Mg_xZnO_{(1-x)}/rGO$ at $x=0.03$ shows four strong peaks correspond to carbon (C), oxygen (O), zinc (Zn) and magnesium (Mg) with 23.72, 30.84, 31.21 and 14.23wt%, respectively. $Mg_xZnO_{(1-x)}/rGO$ at $x=0.06$ shows four strong peaks correspond to carbon (C), oxygen (O), zinc (Zn) and magnesium (Mg) with 37.32, 23.47, 37.56 and 1.65wt%, respectively. $Mg_xZnO_{(1-x)}/rGO$ at $x=0.09$ shows four strong peaks correspond to carbon (C), oxygen (O), zinc (Zn) and magnesium (Mg) with 25.27, 23.72, 48.45 and 1.57wt%, respectively. Where EDAX for rGO/ZnO nanocomposites shows three strong peaks of C, O and Zn with 49.13, 28.92 and 13.28 wt%, respectively and for ZnO shows two strong peaks correspond to oxygen (O) and zinc (Zn) with 52.02 and 47.98 wt%, respectively. The FTIR spectrum of the peaks observed in the spectra at nearly ~ 3685 due to the O-H stretching vibrations, peaks observed at ~ 2860 due to the C-H stretching vibrations, $1596-1545$ due to the C=O stretching vibrations. The band appeared at 1054 cm^{-1} was assigned to the C-N stretching vibration [26]. Generally, the metal oxides give absorption bands below 1000 cm^{-1} , arising due to the inter-atomic vibrations. Further, the strong bands located at 746 and 530 cm^{-1} indicate the stretching vibration mode of Mg-O and Zn-O, respectively, which confirm the formation of $MgZnO/rGO$ nano composites. The optical properties of the prepared $MgZnO/rGO$ samples are characterized by the UV-visible absorption to determine the band gap of the metal oxide nanocomposites. It can be seen in all the spectra that the strong absorption peaks were appeared at around 350 nm , which is attributed to the band gap absorption in $MgZnO$ nanocomposites. The calculated values of the band gap energies of $MgZnO$ nanocomposites are 3.47 , 3.48 and 3.51 eV respectively, at wavelengths 357 nm , 356 nm and 352 nm which are good agreement with reported band gap values of $MgZnO$ nanocomposites. From the UV-vis analysis when the Mg composition is increased we can observe the change in energy band gap and wavelength as the Mg composition increases the band gap energy increases and the wavelength decreases.

References

- [1] Kaveh Movlaee, Mohammad Reza Ganjali, Parviz Norouzi and Giovanni Neri, Iron-Based Nanomaterials/Graphene Composites for Advanced Electrochemical Sensors, *Nanomaterials*, 7 (2017) 1-33.
- [2] Narges Ajami, Juliet Ordoukhanian, Preparation and Characterization of POAP/Fe₂O₃ Magnetic Nanocomposite in One-Step Method, *Int. J. Electrochem. Sci.*, 13 (2018) 424 – 432. ISSN: 2277-9655 [Anandan* et al., 7(8): August, 2018] Impact Factor: 5.164 ICTM Value: 3.00 CODEN: IJESS7 [http:// www.ijesrt.com](http://www.ijesrt.com)© International Journal of Engineering Sciences & Research Technology [498]
- [3] Ibrahim R. Agool, Ahmed Hashim, Preparation of (PVA-PEG-PVP-MgO, CoO) Nanocomposites and Study their Optical Properties, *International Journal of Science and Research*, 3 (2014) 1729-1732.
- [4] Ikim MI, Yu Spiridonova E, Belysheva TV, Gromov VF, Gerasimov GN, Trakhtenberg LI. Structural properties of metal oxide nanocomposites: Effect of preparation method. *Russian Journal of Physical Chemistry B*. 2016;10(3):543-6.
- [5] Greenland DJ, Hayes MHB, editors. *The chemistry of soil processes*. New York: Wiley; 1981
- [6] Geim A.K, Novoselov K.S: *Nat Mater*, Vol. 6 (2007), p.183.
- [7] Williams J.R, DiCarlo L, Marcus C.M: *Science*, Vol. 317 (2007), p.638.
- [8] Service R.F: *Science*, Vol. 324 (2009), p.875.
- [9] Kim K.S, Zhao Y, Jang H, Lee S.Y, Kim J.M, Kim K.S, Ahn J.H, Kim P, Choi J.Y, Hong B.H: *Nature*, Vol. 457 (2009), p.706.
- [10] S. Park, R.S. Ruoff: *Nat. Nanotechnol.*, 4 (2009), pp. 217-224
- [11] O.C. Compton, S.T. Nguyen: *Small*, 6 (2010), pp. 711-723
- [12] Y. Zhu, S. Murali, W. Cai, X. Li, J.W. Suk, J.R. Potts, R.S. Ruoff: *Adv. Mater.*, 22 (2010), pp. 3906-3924
- [13] D. Konios, M.M. Stylianakis, E. Stratakis, E. Kymaki: *J. Colloid Interface Sci.*, 430 (2014), pp. 108-112
- [14] I.K. Moon, J. Lee, R.S. Ruoff, H. Lee: *Nat. Commun.*, 1 (2010), p. 73
- [15] S. Pei, H.M. Cheng: *Carbon* N. Y., 50 (2012), pp. 3210-3228
- [16] S.Y. Toh, K.S. Loh, S.K. Kamarudin, W.R.W. Daud: *Chem. Eng. J.*, 251 (2014), pp. 422-434
- [17] S. Stankovich, D.A. Dikin, R.D. Piner, K.A. Kohlhaas, A. Kleinhammes, Y. Jia, Y. Wu, S.T. Nguyen, R.S. Ruoff: *J. Phys. Chem. C*, 113 (2009), pp. 17330-17335
- [18] Ahuja R, Fast L, Eriksson O, et al. Elastic and high pressure properties of ZnO. *J Appl Phys*. 1998;83:8065–8067.
- [19] Jiahai Bai, Fantao Meng, Chunheng Wei, Yunxia Zhao, Huihui Tan and Juncheng Liu, Solution Combustion Synthesis and Characteristics of Nanoscale MgO Powders.” *Ceramics – Silikáty*, 55(1), pp. 20-25, 2011
- [20] Y. Yang, H. Chen, B. Zhao, X. Bao, Size control of ZnO nanoparticles via thermal decomposition of zinc acetate coated on organic additives *J. Cryst. Growth* 263 (2004) 447-453.
- [21] B.Q. Xu, J.M. Wei, H.Y. Wang, K.Q. Sun, Q.M. Zhu, Nano-MgO: Novel Preparation and Application as Support of Ni Catalyst for CO₂ Reforming of Methane, *Catal. Today* 68 (2001) 217-225.

- [22] M. Purica, E. Budianu, E. Rusu, M. Danila, R. Gavrilă, Optical and structural investigation of ZnO thin films prepared by chemical vapor deposition (CVD), *Thin Solid Films* 403–404 (2002) 485.
- [23] F. Xu, Y.F. Yuan, D.P. Wu, M. ZhO, Z.Y. Gao, K. Jiang, Synthesis of ZnO/Ag/graphene composite and its enhanced photocatalytic efficiency, *Mater. Res. Bull.* 48(2013) 2066-2070.
- [24] C. Xu, X. Wang, J.W. Zhu, X.J. Yang, L. Lu, Deposition of Co₃O₄ nanoparticles onto exfoliated graphite oxide sheets, *J. Mater. Chem.* 18(2008) 5625-5629.
- [25] C. Nethravathi, T. Nisha, N. Ravishankar, C. Shivakumara, M. Rajamathi, Graphene-nanocrystalline metal sulphide composites produced by a one-pot reaction starting from graphite oxide, *Carbon.* 47(2009) 2054-2059.
- [26] X.Y. Yang, X.Y. Zhang, Y.F. Ma, Y. Huang, Y.S. Wang, Y.S. Chen, Superparamagnetic graphene oxide-Fe₃O₄ nanoparticles hybrid for controlled targeted drug carriers, *J. Mater. Chem.* 19(2009) 2710-2714.
- [27] D.H. Wang, D.W. Choi, J. Li, Z.G. Yang, Z.M. Nie, R. Kou, D.H. Hu, C.M. Wang, L.V. Saraf, J.G. Zhang, I.A. Aksay, J. Liu, Self-assembled TiO₂-graphene hybrid nanostructures for enhanced Li-Ion insertion, *ACS Nano.* 3(2009) 907-914.
- [28] S.M. Paek, E. Yoo, I. Honma, Enhanced cyclic performance and lithium storage capacity of SnO₂/graphene nanoporous electrodes with three-dimensionally delaminated flexible structure, *Nano Lett.* 9(2009) 72-75.
- [29] G. Williams, B. Seger, P.V. Kamat, TiO₂-graphene nanocomposites UV-assisted photocatalytic reduction of graphene oxide, *ACS Nano.* 2(2008) 1487-1491.
- [30] T. Cassagneau, J.H. Fendler, S.A. Johnson, T.E. Mallouk, Self-assembled diode junctions prepared from a ruthenium tris (bipyridyl) polymer, n-type TiO₂ nanoparticles, and graphite oxide sheets, *Adv.Mater.* 12(2000) 1363-1366.
- [31] G. Williams, P. V. Kamat, Graphene-semiconductor nanocomposites: excited-state interactions between ZnO nanoparticles and graphene oxide, *Langmuir.* 25(2009) 13869-13873.
- [32] Y. Li, Y. Bando, T. Sato, Preparation of network-like MgO nanobots on Si substrate, *Chem. Phys. Lett.* 359 (2002) 141-145.
- [33] J.H. Lee, K.H. Ko, B.O. Park, Electrical and Optical Properties of ZnO Transparent Conducting Films by the sol-gel method, *J. Cryst. Growth* 247 (2003) 119-125.
- [34] K.F. Cai, E. Mueller, C. Drasar, A. Mroczek, Sol-gel processing of ZnO-coated TiB₂ composite powders, *Mater. Lett.* 57 (2003) 4251.
- [35] H.S. Choi, S.T. Hwang, Magnesium Oxide Nanoparticles Prepared by Ultrasound Enhanced Hydrolysis of Mg-Alkoxides, *J. Mater. Res.* 15 (2000) 842-845.
- [36] T. Lopez, R. Gomez, J. Navarrete, E. Lopez-Salinas, Evidence for Lewis and Brønsted Acid Sites on MgO Obtained by Sol-Gel, *J. Sol-Gel Sci. Technol.* 13 (1998) 1043.
- [37] R. Ayouchi, D. Leinen, F. Martin, M. Gabas, E. Dalchiele, J.R. Ramos-Barrado, Preparation and characterization of transparent ZnO thin films obtained by spray pyrolysis, *Thin Solid Films* 426 (2003) 68-77.
- [38] Y.Q. Zhu, W.K. Hsu, W.Z. Znou, M. Terrones, H.W. Kroto, D.R.W. Walton, Selective Co-catalyzed growth of novel MgO fishbone fractal nanostructures, *Chem. Phys. Lett.* 347 (2001) 337-343.
- [39] Y.C. Hong, H.S. Uhm, Synthesis of MgO nano powder in atmospheric microwave plasma torch, *Chem. Phys. Lett.* 422 (2006) 174-178.
- [40] Z.M. Dang, L.Z. Fan, S.J. Zhao, C.W. Nan, Preparation of nano sized ZnO and dielectric properties of composites filled with nano sized ZnO, *Mater. Sci. Eng. B* 99 (2003) 386-389.
- [41] Q.D. Zhao, M. Yu, T.F. Xie, L.L. Peng, P. Wang, D.J. Wang, Photovoltaic properties of a ZnO nanorod array affected by ethanol and liquid-crystalline porphyrin, *Nanotechnology.* 19(2008) 245706.
- [42] L.Q. Wang, Y. Wu, F.Y. Chen, X. Yang, Photocatalytic enhancement of Mg-doped ZnO nanocrystals hybridized with reduced graphene oxide sheets. *Prog. Nat. Sci.* 24(2014) 6-12.
- [43] Lin Qin Wang, Yan Wu*, Xiang Yang Enhanced Photocatalytic Properties of Ag-Modified Mg-Doped ZnO Nanocrystals Hybridized with Reduced Graphene Oxide Sheets DOI: <https://doi.org/10.4028/www.scientific.net/MSF.814.161> Materials Science Forum (Volume 814)
- [44] A. Ohtomo, M. Kawasaki, T. Koida, K. Masubuchi, and H. Koinuma, cMgxZn1-xOMgxZn1-xO as a II-VI widegap semiconductor alloy, *Appl. Phys. Lett.* 72 (1998) 2466.
- [45] T. Minemoto, T. Negami, S. Nishiwaki, H. Takakura, Y. Hamakawa, Preparation of Zn1-xMgxO films by radio frequency magnetron sputtering, *Thin Solid Films* 372 (2000) 173-176.
- [46] S. Choopun, R.D. Vispute, W. Yang, R.P. Sharma, T. Venkatesan, Realization of band gap above 5.0 eV in metastable cubic-phase MgxZn1-xOMgxZn1-xO alloy films, *Appl. Phys. Lett.* 80 (2002) 1529.
- [47] J. Song, X. Wang and C.-T. Chang, *J. Nanomater.*, 2014, 2014, 1-6, doi: 10.1155/2014/276143.
- [48] H. R. Wang, K. M. Chen, Preparation and surface active properties of biodegradable dextrin derivative surfactants, *Colloids and Surfaces A : Physicochem. Eng.Aspects* 281, (2006) 190-193.
- [49] S. Chawla, K. Jayanthi, H. Chander, D. Haranath, S.K. Halder, M. Kar, Synthesis and optical properties of ZnO/MgO nanocomposite, *Journal of Alloys and Compounds* 459, (2008) 457–460.
- [50] G.Kasi, K.Vishwanathan, K.Sadeghi, J.Seo, Optical, thermal, and structural properties of polyurethane in Mg-doped zinc oxide nanoparticles for antibacterial activity. *Prog.Org.Coat.* 133,309-315(2015)
- [51] L.S.Rao, T.V.Rao, S.Naheed, P.V.Rao, Structural and optical properties of zinc magnesium oxide nanoparticles synthesized by chemical co-precipitation. *Mater.Chem.Phys.* 203,133-140(2018)
- [52] Synthesis and characterization of urea doped MgZnO nanoparticles for electronic applications Nacer Badi1, 2 · Syed Khasim1,2,3 · Apsar Pasha Springer-Verlag GmbH

- Germany, part of Springer Nature 2019 Applied Physics A (2019) 125:851 <https://doi.org/10.1007/s00339-019-3149-9>
- [53] M. Xie, D. Zhang, Y. Wang and Y. Zhao, Colloids Surf. A Physicochem. Eng. Asp., 2020, 603, 125247, doi: 10.1016/j.colsurfa.2020.125247
- [54] G. Kasi, K. Viswanathan, K. Sadeghi, J. Seo, Optical, thermal, and structural properties of polyurethane in Mg-doped zinc oxide nanoparticles for antibacterial activity. Prog. Org. Coat. 133, 309–315 (2019)
- [55] Y. Yokomizo, S. Krishnamurthy, P.V. Kamat., Catal. Today 199 (2013) 36–41
- [56] Y. Wu, J. Yun, L.Q. Wang, X. Yang, Cryst. Res. Technol. 48 (2013) 145–152